Inducible glutathione S-transferase (IrGST1) from the tick Ixodes ricinus is a haem-binding protein

Perner, Jan; Kotál, Jan; Hatalová , Tereza; Urbanová , Veronika; Bartošová-Sojková, Pavla; Brophy, Peter; Kopáček, Petr

Published in:
Insect Biochemistry and Molecular Biology

DOI:
10.1016/j.ibmb.2018.02.002

Publication date:
2018

Citation for published version (APA):
Perner, J., Kotál, J., Hatalová , T., Urbanová , V., Bartošová-Sojková, P., Brophy, P., & Kopáček, P. (2018). Inducible glutathione S-transferase (*Ir*GST1) from the tick *Ixodes ricinus* is a haem-binding protein. *Insect Biochemistry and Molecular Biology*, *95*, 44-54. https://doi.org/10.1016/j.ibmb.2018.02.002

Accepted Manuscript

Inducible glutathione S-transferase (*Ir*GST1) from the tick *Ixodes ricinus* is a haem-binding protein

Jan Perner, Jan Kotál, Tereza Hatalová, Veronika Urbanová, Pavla Bartošová-Sojková, Peter M. Brophy, Petr Kopáček

PII: S0965-1748(18)30021-3

DOI: 10.1016/j.ibmb.2018.02.002

Reference: IB 3035

To appear in: *Insect Biochemistry and Molecular Biology*

Received Date: 19 January 2018

Revised Date: 14 February 2018

Accepted Date: 19 February 2018

Please cite this article as: Perner, J., Kotál, J., Hatalová, T., Urbanová, V., Bartošová-Sojková, P., Brophy, P.M., Kopáček, P., Inducible glutathione S-transferase (*Ir*GST1) from the tick *Ixodes ricinus* is a haem-binding protein, *Insect Biochemistry and Molecular Biology* (2018), doi: 10.1016/j.ibmb.2018.02.002.

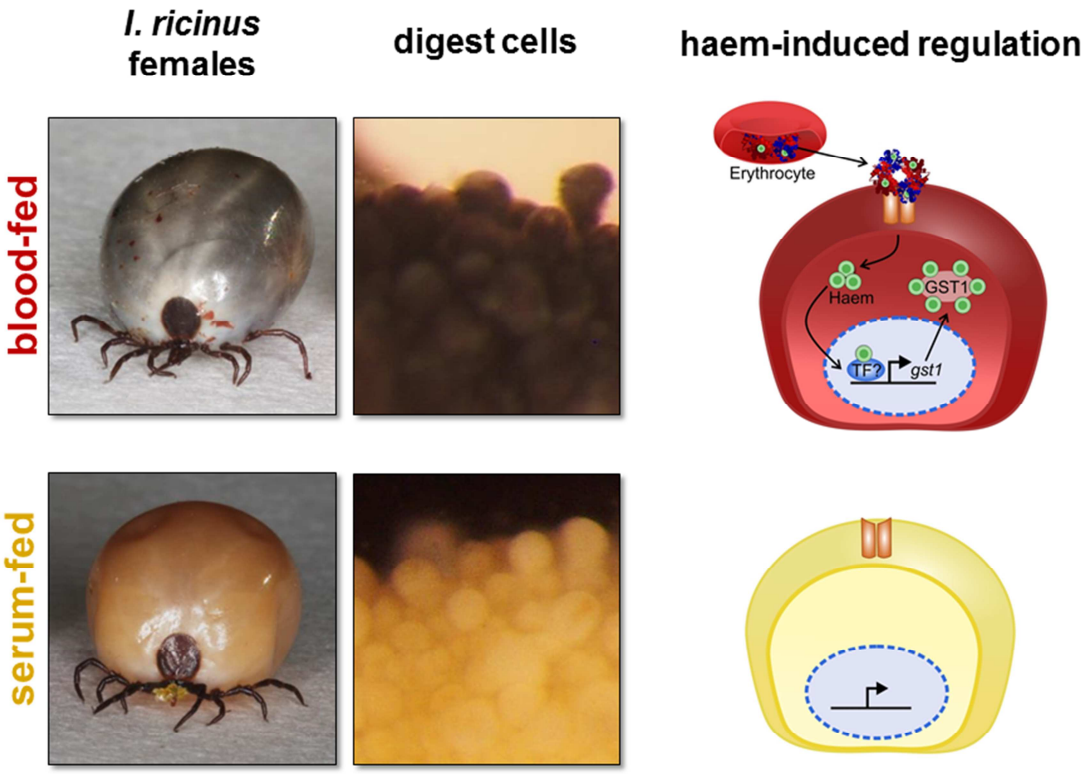

Inducible glutathione S-transferase (*Ir*GST1) from the tick *Ixodes ricinus* is a haem-binding protein

Jan Perner[a,b]*, Jan Kotál[a,b], Tereza Hatalová[b], Veronika Urbanová[a], Pavla Bartošová-Sojková[a], Peter M. Brophy[c], Petr Kopáček[a]

[a] *Institute of Parasitology, Biology Centre of the Czech Academy of Sciences, Branišovská 31, 370 05, České Budějovice, Czech Republic*

[b] *Faculty of Science, University of South Bohemia, Branišovská 31, 370 05, České Budějovice, Czech Republic*

[c] *Institute of Biological, Environmental and Rural Sciences (IBERS), Aberystwyth University, Aberystwyth, SY23 3DA, UK*

Abstract

Blood-feeding parasites are inadvertently exposed to high doses of potentially cytotoxic haem liberated upon host blood digestion. Detoxification of free haem is a special challenge for ticks, which digest haemoglobin intracellularly. Ticks lack a haem catabolic mechanism, mediated by haem oxygenase, and need to dispose of vast majority of acquired haem *via* its accumulation in haemosomes. The knowledge of individual molecules involved in the maintenance of haem homeostasis in ticks is still rather limited. RNA-seq analyses of the *Ixodes ricinus* midguts from blood- and serum-fed females identified an abundant transcript of *glutathione S-transferase* (*gst*) to be substantially up-regulated in the presence of red blood cells in the diet. Here, we have determined the full sequence of this encoding gene, *ir-gst1*, and found that it is homologous to the delta-/epsilon-class of GSTs. Phylogenetic analyses across related chelicerates revealed that only one clear *Ir*GST1 orthologue could be found in each available transcriptome from hard and soft ticks. These orthologues create a well-supported clade clearly separated from other ticks' or mites' delta-/epsilon-class GSTs and most likely evolved as an adaptation to tick blood-feeding life style. We have confirmed that *Ir*GST1 expression is induced by dietary haem(oglobin), and not by iron or other components of host blood. Kinetic properties of recombinant *Ir*GST1 were evaluated by model and natural GST substrates. The enzyme was also shown to bind haemin *in vitro* as evidenced by inhibition assay, VIS spectrophotometry, gel filtration, and affinity chromatography. In the native state, *Ir*GST1 forms a dimer which further polymerises upon binding of excessive amount of haemin molecules. Due to susceptibility of ticks to haem as a signalling molecule, we speculate that the expression of *Ir*GST1 in tick midgut functions as intracellular buffer of labile haem pool to ameliorate its cytotoxic effects upon haemoglobin intracellular hydrolysis.

1. Introduction

Ticks are blood-feeding ectoparasites notorious for transmitting a wide variety of infection diseases of humans as well as farm and companion animals (de la Fuente et al., 2008). Hard ticks (Ixodidae) undergo a life cycle of three parasitic stages - larvae, nymphs, and adults, each of which requires one blood meal as the only source of nutrients for their further development and reproduction. Adult hard tick females imbibe large quantities of host blood exceeding up to hundred times their unfed weight. The blood meal is ultimately processed into the huge clutch of eggs before the female dies (Sonenshine and Roe, 2014). The proteinaceous components of the blood meal are internalised by tick digest cells lining up the midgut epithelium. The host proteins are then hydrolysed intracellularly, in the endo-lysosomal system consisting of a network of acidic cysteine and aspartic peptidases (Sojka et al., 2013). Haemoglobin degradation is inevitably concomitant with the intracellular release of haem, a pro-oxidative molecule, which is potentially cytotoxic when in excess (Graca-Souza et al., 2006).

We have recently demonstrated that ticks lost genes encoding enzymes involved in both haem biosynthesis and haem degradation (Perner et al., 2016a). Instead, ticks acquire haem exogenously, from the host haemoglobin (Perner et al., 2016a). A small portion of acquired haem is further dispatched for systemic inter-tissue distribution to allow assembly of endogenous haemoproteins, while most of the haem has to be disposed by effective means of detoxification. In contrast to haemozoin formation, a well-described mechanism of haem disposal in malaric plasmodium, schistosomes, or rhodnius vectors, ticks accumulate excessive haem as non-crystalline aggregates, in a specialised organelles generally referred to as haemosomes (Lara et al., 2005; Lara et al., 2003). Haem intracellular transport from digestive vesicles to cytosol was reported to be mediated by an ATP-binding cassette (ABCB10) (Lara et al., 2015). However, the next fate of cytosolic haem is still poorly understood.

In order to contribute to the knowledge of haem metabolism in ticks, we have tested, by RNA-seq analyses, which transcripts change their levels in response to the presence of red blood cells (RBCs) in the tick diet. For this purpose, we compared the transcriptomes of midguts from *I. ricinus* females membrane-fed either bovine blood or bovine serum. Among the surprisingly low number of transcripts with decreased or elevated levels in response to RBCs presence, we identified a gut-specific transcript Ir-114935 encoding a delta-/epsilon-class glutathione S-transferase (Perner et al., 2016b).

Members of the glutathione S-transferases (GSTs) family are ubiquitously present in eukaryotic organisms where they serve mainly in cellular detoxification of endogenous or xenobiotic compounds *via* their conjugation with the reduced glutathione (GSH), which results in their increased water solubility and excretion (Townsend and Tew, 2003; Wilce and Parker, 1994). Based on their organismal origin, primary sequence, substrate specificity, immunological, or chromosomal localisations, the GSTs can be grouped into more than a dozen classes historically tagged by Greek letters (Mashiyama et al., 2014). The

availability of the tick *Ixodes scapularis* genome (Gulia-Nuss et al., 2016) made it possible to enumerate and classify GSTs encoded in this species (Reddy et al., 2011). Out of 35 identified *Is*GST genes, 32 encoded cytosolic GSTs comprising 14 genes of vertebrate/mammalian Mu-class, 7 genes of Delta- and 5 genes of Epsilon- classes specific for insects, and 3 genes each were of common Omega- and Zeta- classes (Reddy et al., 2011). Given their capability to detoxify xenobiotics, GSTs have a well-established role in development of insecticide resistance in insect pests (for review see e.g. (Enayati et al., 2005) or acaricide resistance in ticks (Dreher-Lesnick et al., 2006; Duscher et al., 2014; He et al., 1999; Vaz et al., 2004a)). However, much less is known about the house-keeping physiological function of GSTs in the management of potentially toxic endogenous haem originating from the blood meal diet of the haematophagous parasites.

In this work, we provide a biochemical and functional characterisation of the haem(oglobin)-inducible GST from *I. ricinus* (further referred to as *Ir*GST1) and demonstrate that this enzyme is capable to efficiently bind haemin *in vitro*. Clear orthologues of *Ir*GST1 could be found only in other tick species, but not in other organisms, suggesting that *Ir*GST1 represents a novel class of tick-specific GSTs that evolved during the adaptation of ticks to their blood-feeding life style.

2. Materials and methods

2.1. *Tick maintenance and natural feeding*

Adult *I. ricinus* ticks were collected in the forest near České Budějovice. Ticks were kept at 24 °C and 95% humidity under a 15:9-hour day/night regime. All laboratory animals were treated in accordance with the Animal Protection Law of the Czech Republic No. 246/1992 Sb., ethics approval No. 357 095/2012. The study was approved by the Institute of Parasitology, Biology Centre of the Czech Academy of Sciences (CAS) and Central Committee for Animal Welfare, Czech Republic (protocol no. 1/2015).

2.2. *Tick membrane feeding*

Membrane feeding of ticks was performed using a stationary six-well plate format according to Thomas Kröber and Patrick Guerin (Kröber and Guerin, 2007). Whole bovine blood was collected in a local slaughter house and manually defibrinated. To obtain serum, whole blood samples were centrifuged at 2500 × g, 10 min, 4°C and the resulting supernatant was collected and centrifuged again at 10 000 × g, 10 min, 4°C. Fifteen females were placed in a feeding unit lined with a thin (80–120 μm) silicone membrane, previously pre-treated with a bovine hair extract in dichloromethane (0.5 mg of low volatile lipids). After 24 hr, unattached or dead females were removed and an equal number of males were added to the attached females into the feeding unit. Diets were exchanged in a 12h regime, with concomitant

addition of 1 mM adenosine triphosphate (ATP) and gentamicin (5 µg/ml). For diet supplementation, pure bovine haemoglobin (Sigma - H2500), bovine holo-Transferrin (Rocky Mountain Biologicals), and haemin (Sigma - H9039) was used. For membrane feeding experiments, haemin stock solution (62.5 mM haemin dissolved in 100 mM NaOH), was diluted 100× to reach 625 µM (final concentration) equalling a haem equimolarity with 1% haemoglobin (w/v).

2.3. Tissue dissection, RNA extraction, cDNA synthesis, and RT-qPCR

Membrane-fed *I. ricinus* females were forcibly removed from the membrane on day 6 of feeding. Tick midguts were dissected on a paraplast-filled Petri dish under a drop of ice-cold DEPC-treated PBS. Total RNA was isolated from dissected tissues using a NucleoSpinRNA II kit (Macherey-Nagel, Germany), quality checked by gel electrophoresis on agarose gel, and stored at -80°C prior to cDNA synthesis. cDNA preparations were made from 0.5 µg of total RNA in independent triplicates using the Transcriptor High-Fidelity cDNA Synthesis Kit (Roche Diagnostics, Germany). The cDNA served as templates for subsequent quantitative expression analyses by RT-qPCR. Samples were analysed by a LightCycler 480 (Roche) using Fast Start Universal SYBR Green Master Kit (Roche). Relative expressions were calculated using the ΔΔCt method (Pfaffl, 2001). The expression profiles were normalised to *I. ricinus* elongation factor 1α (*ef-1α*). List of primers is available as Supplementary Table S1.

2.4. Sequencing, cloning, and phylogenetic analysis of IrGST1

Full cDNA sequence of gene encoding *Ir*GST1 was amplified using primers derived from 5'- and 3'-untranslated regions of the orthologous *I. scapularis* gene (ISCW005803) (Supplementary Table S1). *I. ricinus* midgut-specific cDNA prepared from midguts of females fed for 3 days served as template. The amplified 786 bp long PCR product was cloned into a pCR4-TOPO TA vector (Invitrogen) and sequenced. Amino acid sequences of *Ir*GST1 and other selected delta-/epsilon-class GSTs were aligned using the E-INS-i algorithm in MAFFT v7.017 (Katoh et al., 2002) and manually trimmed in Geneious v8.1.3. (Kearse et al., 2012) to the final length of 221 amino acids. Maximum parsimony analysis was performed in PAUP* v4.b10 (Swofford, 2003) using a heuristic search with random taxa addition, the ACCTRAN option, TBR swapping algorithm, all characters treated as unordered and gaps treated as missing data. Maximum-likelihood analysis was performed in RAxMLv7.2.8 (Stamatakis, 2006) under the PROTGAMMABLOSUM62 + Γ model. Mosquitoes *Anopheles gambiae* and *Aedes aegypti* were used as outgroups. Bootstraps were based on 1000 replicates for both analyses. Bayesian inference analysis was performed in MrBayes v3.0 (Ronquist and Huelsenbeck, 2003) using the WAG + Γ model of evolution. Analyses were initiated with random starting trees, four simultaneous MCMC chains sampled at intervals of 200 trees and posterior probabilities estimated from 1 million generations (burn-in 100 000).

2.5. Expression and purification of recombinant polyhistidine-tagged and untagged IrGST1

Poly-histidine tagged recombinant *Ir*GST1 was prepared by amplification of a coding sequence using *ir-gst1*-specific primers (Supplementary Table S1) and the 694 bp product was cloned into a pet100 vector (Invitrogen) following manufacturers' protocol. Resulting plasmid was transformed into TOP10 *E. coli* cells and positive clones were selected on ampicillin LB plates, sequenced, and transformed into *E. coli* BL21 Star (DE3) chemically competent cells (Invitrogen). Cells were grown in ampicillin LB medium at 37°C and when reached OD = 1.6, the culture was induced with 0.1 mM isopropyl β-D-1-thiogalactopyranoside (IPTG). The cells were cultured for 6 h and the harvested cells were suspended in PBS and homogenised using sonication. The centrifuged homogenate was loaded on a Ni^{2+}-IMAC agarose (GE Healthcare) and the resin was washed with 20 bed volumes of 20 mM phosphate buffer pH 6.0, 0.5 M NaCl, 20 mM imidazol, 10% glycerol and 0.5% Triton X-100 (v/v) to remove non-specifically bound proteins. The recombinant protein was then eluted from the resin by 100 mM imidazole in a washing buffer, concentrated and transferred to the PBS by ultrafiltration using 15 ml centrifuge filter units (cut-off 10 kDa, Merck Millipore). The monospecific polyclonal antibodies against *Ir*GST1 were raised in rabbits as previously described (Grunclova et al., 2006) and used for Western blotting. A PCR product encoding an untagged recombinant *Ir*GST1 was amplified using the same primer pair (with the reverse primer containing a stop codon), cloned into the pet101 vector (Invitrogen), and further expressed in *E. coli* as described above. The cell pellet was homogenised in a tenth of original culture volume in 20 mM Tris pH 8.5 and centrifuged at 10 000 × g, 20 min, 4°C. The supernatant was filtered through a 0.22 μm filter (Merck Millipore) and applied on MonoQ HR 5/5 column (GE Healthcare) using an AKTA pure chromatographic system (GE Healthcare). The sample was separated at 1 ml/min flowrate in 20 mM Tris pH 8.5 and eluted by a 0–500 mM NaCl gradient. The fractions with enriched GST activity (see bellow) were pooled, concentrated by ultrafiltration (10 kDa cut-off), applied onto Superdex 75 10/300 GL column (GE Healthcare) and further separated at 1 ml/min flowrate in 20 mM Tris pH 8.5, 150 mM NaCl. Gel filtration molecular standards (ferritin, aldolase, serum albumin, and chymotrypsinogen A) were used for molecular weight determination. Purified *Ir*GST1 was used for immunising mice and the mice immune sera were used for immunohistochemistry (see below).

2.6. Reducing SDS-PAGE and Western blot analysis

Tick midgut homogenates were prepared in 1% Triton X-100 in PBS supplemented with a Complete™ cocktail of protease inhibitors (Roche) using a 29G syringe needle, and subsequently subjected to three freeze/thaw cycles using liquid nitrogen. Proteins were then extracted for 1 hr at 4°C and 1 200 rpm using a Thermomixer comfort (Eppendorf, Germany). Samples were then centrifuged 15 000 × g, 10 min, 4°C and separated by reducing SDS-PAGE on 12.5 % polyacrylamide gels. Protein profiles were visualized

using TGX stain-free chemistry (BioRad) or by staining with Coomassie Brilliant Blue R-250 (CBB). Proteins were transferred onto Immun-Blot® LF PVDF membrane using a Trans-Blot Turbo system (BioRad). For Western blot analyses, membranes were blocked in 3% (w/v) non-fat skimmed milk in PBS with 0.05% Tween 20 (PBS-T), incubated in immune serum (α*Ir*GST1) diluted in PBS-T (1:5000) or in immune serum against *I. ricinus* ferritin 1 (α*Ir*Fer1) diluted in PBS-T (1:50). The goat anti-rabbit IgG-peroxidase antibody (Sigma A9169) diluted in PBS-T (1:50000) was used as a secondary antibody. Signals were detected using ClarityWestern ECL substrate, visualized using a ChemiDoc MP imager, and analysed using Image Lab Software (BioRad).

2.7. Substrate specificities of IrGST1 and isoelectric focusing

The substrate specificities of *Ir*GST1 were tested with known model and natural substrates of GSTs (Morphew et al., 2012). In brief, enzyme assays were measured using a UV/VIS Gilford Response spectrophotometer over 3 min at 25°C. Glutathione S-transferase (GST) activity was determined using the model substrate 1-chloro-2,4-dinitrobenzene (CDNB) according to the method described by Habig et al. (Habig et al., 1974). The enzyme assay was performed in 100 mM potassium phosphate buffer pH 6.5, containing 1mM reduced glutathione (GSH) and 1mM CDNB at 340 nm (ε = 9.6 x 106 cm^{-2} mol^{-1}). GSH-dependent peroxidase activity of *Ir*GST1 was determined using cumene hydroperoxide (the model lipid hydroperoxide substrate)(Jaffe and Lambert, 1986). The assay was carried out in 50 mM phosphate buffer pH 7.0 containing 1 mM GSH, 0.2 mM NADPH, 0.5 U glutathione reductase (Sigma, G3664), and 1.2 mM cumene hydroperoxide. The reaction was measured at 340 nm (ε = 6.22 x 106 cm^{-2} mol^{-1}). GST activity with trans-2-nonenal was determined as previously described (Brophy et al., 1989) The reaction mix was composed of 100 mM potassium phosphate buffer pH 6.5, 1 mM GSH, and 0.23 mM trans-2-nonenal and the enzymatic activity was measured at 225 nm (ε = -19.2 x 106 cm^{-2} mol^{-1}). Isoelectric focusing (IEF) was performed on IEF precast gels (BioRad) and separated by IEF cathode buffer 2mM lysine (free base), 2 mM arginine (free base) and IEF anode buffer 0.7 mM phosphoric acid at increased voltage modes: 100 V 60 min, 250 V 60 min, 500 V 30 min. IEF markers of pI range 3–10 were used (SERVA 39212.01).

2.8. Determination of kinetic parameters and inhibition studies

The determination of *Ir*GST1 apparent Michaelis constants to CDNB and GSH as substrates were performed in triplicates, with varying concentrations of CDNB and constant GSH (1 mM), or constant CDNB (1 mM) and varying concentrations of GSH, respectively. Kinetic constants were calculated by non-linear regression analysis of the experimentally measured activities. Data were fitted to the Michaelis-Menten equation using GraphPad Prism 6.0 software. The inhibition of *Ir*GST1 by haem-related

compounds was investigated by CDNB activity assay with haemin (haem-chloride), haematin (haem-hydroxide, Sigma H3281), protoporphyrin IX (PPIX) (Sigma P8293), and myoglobin (Sigma M0630). Haemin and haematin were dissolved in 100 mM NaOH, PPIX in DMSO, and myoglobin in H_2O.

2.9. Examination of haemin-IrGST1 binding by spectrophotometry and haemin-affinity chromatography

The absorption properties of haemin in the presence of *Ir*GST1 were measured by recording the absorption spectra in the range from 300 nm to 450 nm using a UV-1800 spectrophotometer (Shimadzu). Constant concentration of haemin (10 µM) in 20 mM sodium phosphate buffer (pH 8.0), 50 mM NaCl was incubated for 15 min with different concentrations of *Ir*GST1 corresponding to the molar ratios of r-*Ir*GST1: haemin from 0 to 2.

Binding of *Ir*GST1 to the commercial haemin-agarose (Sigma H6390) was examined using a pull down experiment. *E. coli* expressing *Ir*GST1 (see above) were homogenised in 1.5 ml of 50 mM Tris-HCl pH 8.0, 0.5 M NaCl (Tris-NaCl buffer), centrifuged and the supernatant was incubated with 50 µl of haemin-agarose for 1 h with slow rotation. Agarose beads were then allowed to settle, supernatant removed, and the agarose was then transferred to an empty column (BioRad) and extensively washed with Tris-NaCl buffer. Specifically bound proteins were then eluted with 1 M urea in Tris-NaCl buffer and separated using SDS-PAGE. Coomassie-stained protein band was excised and prepared for mass fingerprint analysis. Briefly, the excised gel was incubated with 50 mM ammonium bicarbonate: 100% acetonitrile (1:1) solution for 15 minutes at 37°C to destain the gel. The gel was dehydrated in 100% acetonitrile for 30 minutes at 37°C and subsequently rehydrated in trypsin solution (100 ng/µl) in ammonium bicarbonate, left for 45 minutes at 8°C, and incubated at 37°C over-night. Supernatant was removed and the gel was washed several times alternately with acetonitrile and 50 mM ammonium bicarbonate. Samples were then vacuum-dried, resuspended 1% formic acid (w/w) and analysed by LC MS/MS on an Agilent 6550 iFunnel Q-TOF mass spectrometer with a Dual AJS ESI source coupled to a 1290 series HPLC system (Agilent, Cheshire, UK) according to Morphew et al. 2014 (Morphew et al., 2014).

2.10. Haemin binding size exclusion chromatography

Haemin binding size exclusion chromatography was performed with *Ir*GST1, diluted to 35 µM (0.9 mg/ml) in 20 mM Tris pH 8.5, 150 mM NaCl. Different molar ratios of haemin (stock solution 35 mM haemin in 100 mM NaOH) were added to 1 ml of *Ir*GST1 solution and incubated for 30 minutes, 250 rpm, 22°C in ThermoMixer® (Eppendorf). Then 250 µl of the membrane filtered (0.22 µm) incubation reaction was separated using Superdex 75 10/300 GL column (GE Healthcare) at 1 ml/min flow rate in 20 mM Tris pH 8.5, 150 mM NaCl and the absorbance was monitored at the dual wavelengths of 280 and 400 nm.

2.11. RNA interference and immunohistochemistry

dsRNA of *ir-gst1* or *gfp* (green fluorescent protein) used for control were synthesised using the MEGAscript T7 transcription kit (Ambion, Lithuania) according to the previously described protocol (Hajdušek et al., 2009). *I. ricinus* females were injected into the haemocoel through to the coxae with *ir-gst1*-specific dsRNA or control *gfp* dsRNA (0.5 µl; 3 µg/µl) using a microinjector (Narishige), allowed to rest for one day and then fed naturally for 5 days on guinea pigs. The efficiency of RNA-mediated silencing *ir-gst1* gene expression was verified at the protein level by Western blot analysis using α*Ir*GST1 antibodies. The visualisation of authentic *Ir*GST1 by indirect immune-fluorescent microscopy in the dissected *I. ricinus* guts was performed as described earlier (Franta et al., 2010) with some modification. Briefly, the semi-thin sections were cut, transferred onto glass slides, and blocked with 1% BSA and 10% goat serum PBS-T (0.3% Triton X-100) for 1 h. Incubation with the primary α*Ir*GST1 antibody (1:100) in PBS-T was performed in a humid chamber for 1.5 h at room temperature. For negative control experiments, the primary antibody incubation was omitted (not shown). Sections were washed with PBS-T (four times 5 min) and then incubated with Alexa Fluor® 488 secondary dye-conjugated goat anti-mouse (Invitrogen/Molecular Probes) diluted to 1:500 in PBS-T for 1 h at room temperature. After washing with PBS-T, the slides were counterstained with DAPI (4',6'-diamidino-2-phenylindole; 2.5 µg/ml; Sigma) for 5 min. Finally, sections were mounted in Fluoromount (Sigma-Aldrich) and examined using the fluorescence microscope BX 53. The semi-thin sections stained with toulidine blue were examined under the light mode of the microscope BX53. The same protocol was carried out for immunodetection of 4-hydroxynonenal (4-HNE) using the commercial rabbit α4-HNE antibody (Abcam ab46545, 1:300) and the 1:500 diluted Alexa Fluor® 488-labeled secondary goat anti-rabbit antibody (Invitrogen/Molecular Probes).

3. Results

3.1. IrGST1 sequence identification and phylogenetic analysis

The transcript Ir-114935, previously shown to be significantly up-regulated in the midguts of blood-fed compared to serum-fed ticks (Perner et al., 2016b), encodes a partial sequence of a putative delta-/epsilon-class glutathione S-transferase. The partial sequence was clearly orthologous to *I. scapularis* ISCW005803 gene encoding delta-class GST, *Is*GSTD2 (Reddy et al., 2011), with 98% sequence identity at both amino-acid and nucleotide levels. The full coding sequence of *Ir*GST1 (deposited in the GenBank under Access. No. MF984398) was obtained by cloning and sequencing of a 786 bp long PCR product amplified using the primers derived from 5'- and 3'-UTR regions of *I. scapularis Is*GSTD2. All performed phylogenetic analyses have unambiguously revealed the *Ir*GST1 orthologues of delta-/epsilon-

class from other hard and soft tick species that create a well-supported clade (Fig. 1A). This specific clade is distinct from the clades of other delta-/epsilon- class GSTs from *I. scapularis*, horseshoe crab, and mites (Fig. 1A), which display much lower sequence identity to *Ir*GST1 (below 50%) (Fig. 1B and Supplementary Fig. S1). The typical SNAIL/TRAIL signature motif present in GSTs of various classes is conserved within the *Ir*GST1 orthologous group as SRAI(A/G). All ticks and mites delta-/epsilon-class GSTs possess a conserved tyrosine residue at the position 6 (Fig. 1B and Supplementary Fig. S1) classifying the enzymes into Y-type major subgroup of cytosolic GSTs (Atkinson and Babbitt, 2009).

3.2. Expression of IrGST1 in the tick gut is inducible by haemin

Even though we have previously demonstrated by RNA-seq and qRT-PCR that expression of contig Ir-114935 encoding *Ir*GST1 is up-regulated in ticks fed on the whole blood (Perner et al., 2016b), a question remaining to be solved was which constituent of red blood cells is responsible for the up-regulation of the *ir-gst1* gene. In order to reveal that, we have conducted a membrane feeding experiment where the ticks were allowed to feed for 5 days haemoglobin-free serum, haemoglobin-free serum supplemented either with 1% w/v bovine haemoglobin, 625 µM haemin (haemin solubilised in sodium hydroxide), mock (sodium hydroxide, 1 mM final concentration), whole blood reconstituted with red blood cells. RT-qPCR analysis revealed that *ir-gst1* is up-regulated by dietary haemin as well as by haemoglobin (Fig. 2A). The up-regulation was observed higher for dietary haemin (unbound or secondarily complexed with albumin) compared to dietary haemoglobin, when the concentration of haem were equimolar. The consistent result was obtained at the protein level, as evidenced by Western blot analysis (Fig. 2B). The levels of *Ir*GST1 in the midgut were dose-dependent on the amount of haemin added to the serum diet and gradually increased from micromolar dietary concentration to 625 µM representing about 1/150 of the physiological concentration of haem present in the whole blood (~ 10 mM) (Fig. 2C). This result indicates that *Ir*GST1 inducibility by host haem may serve as a very sensitive sensor of the blood meal uptake. To confirm that *Ir*GST1 expression is induced exclusively by haem and not by iron, we performed a membrane feeding experiment where ticks were fed diets enriched with bovine holo-transferrin and bovine haemoglobin, known tick sources of iron and haem, respectively (Perner et al., 2016a). We confirmed that while ticks fed transferrin-enriched diet had elevated levels of *Ir*Fer1, *Ir*GST1 levels remained unaltered. Conversely, ticks fed haemoglobin enriched diet had elevated levels of *Ir*GST1 and unaltered levels of *Ir*Fer1 (Fig. 2D). These results underscore that haem and iron sensing in the tick midgut are independent processes.

3.3. RNAi effectively silences the expression of IrGST1 throughout the tick feeding

To study a physiological role of *Ir*GST1 *in vivo*, a knock-down of this transcript was obtained by RNAi-mediated silencing. A confirmation of clear down-regulation of *Ir*GST1 in tick midgut throughout the

feeding was evidenced by Western Blotting (Fig. 3A). Indirect immune-fluorescence microscopy using α*Ir*GST1 antibody confirmed a substantial decrease of fluorescent signal in the maturated midgut digest cells of *Ir*GST1-KD females compared to the control ticks injected with *gfp* dsRNA (Fig. 3B). However, this reduction of *Ir*GST1 in tick midgut digest cells had no obvious impact on the tick feeding and fecundity. *Ir*GST1-KD females could accomplish feeding, reached comparable engorged weights, laid egg clutches of comparable size and colour that gave rise to viable larvae similarly as the control *gfp* group (Fig. 3C, D). GSTs are also known to conjugate GSH to 4-hydroxynonenal (4-HNE), that is a toxic product of lipid peroxidation and a biomarker of oxidative stress (Awasthi et al., 2004; Cheng et al., 2001). The presence of 4-HNE inside the digest cells was detected by indirect immune-fluorescent microscopy. However, no difference of fluorescent intensity was observed in guts from *Ir*GST1-KD and control females (Supplementary Fig. S2), suggesting that *Ir*GST1 is not involved in 4-HNE detoxification. Given the absence of any *Ir*GST1-KD phenotype, we further focused on *in vitro* characterisation of recombinant *Ir*GST1.

3.4. Preparation and enzymatic characterisation of recombinant IrGST1

Recombinant *Ir*GST1 was first expressed in *E. coli* expression system as a His-tagged protein with a theoretical mass 29721 Da and purified in a soluble form from the bacterial lysate using Ni^{2+}-IMAC chromatography under native conditions (Fig. 4A). *E. coli* expressed *Ir*GST1 was active in GSH transferase activity assay using a model substrate 1-chloro-2,4-dinitrobenzene (CDNB) (Fig. 4B). The crude extract of *E. coli* cells had a specific enzymatic activity of 201 ± 13 nmol CDNB/min/mg protein that following elution and dialysis increased to 1820 ± 77 nmol CDNB/min/mg protein in the purified fraction with Km for GSH to be 0.87 ± 0.13 mmol and Km for CDNB to be 2.9 ± 0.64 mmol (Supplementary Fig S3). Despite the capacity to utilise GSH in a CDNB activity assay (Km values for GSH and CDNB were comparable to other reported GSTs (Al-Qattan et al., 2016)), the effort to purify *Ir*GST1 from *E. coli* crude extract or further purify the *Ir*GST1 (IMAC purified) using GSH- or S-hexyl GSH-Sepharose failed given the low binding affinity to these sorbents (Supplementary Fig. S3).

GSTs display a wide range of enzymatic activities with model substrates (Brophy et al., 1990). To reveal the kinetic parameters of *Ir*GST1, assays with typical GST substrates were also carried out using another invertebrate recombinant GST (*Fasciola gigantica* sigma GST) as a control (Morphew et al., 2012). Beside the above mentioned GSH-conjugating activity using CDNB as a model substrate, the *Ir*GST1 exerted also peroxidase activity with the model lipid hydroperoxide substrate - cumene hydroperoxide (Fig. 4B). *Ir*GST1 had no activity towards reactive carbonyls, in contrast to sigma-class *F. gigantica*, GST as assayed using trans-2-nonenal as a natural substrate derived from lipid peroxidation (Brophy et al., 1989) (Fig. 4B).

As several GSTs from different blood feeding parasites have been reported to bind haemin (see below), we have performed a haemin interaction/inhibitory assay of *Ir*GST1 GSH-conjugating activity and compared it to the *Fg*GST over a range of CDNB substrate concentration (Fig. 4C). This experiment revealed that *Ir*GST1 activity is much more sensitive to haemin than *Fg*GST. In order to determine more precisely the inhibition constant of haemin (Ki) for *Ir*GST1, a Dixon plot of inhibitory activities was used and Ki of haemin was determined to be 42 ± 15 nM, indicating a strong binding affinity for *Ir*GST1 (Fig. 4D). Using the CDNB activity assay, we further examined whether free haem, protein-bound haem, or iron-free protoporphyrin IX (PPIX) is responsible for the inhibition of *Ir*GST1. Both free haemin (haem-chloride) and haematin (haem-hydroxide) inhibited the *Ir*GST1 activity with apparent IC_{50} around 200 nM, whereas myoglobin-bound haem or iron-free protoporphyrin IX (PPIX) did not induce any inhibition at the concentration range up to 1 µM (Fig. 4E).

3.5. Recombinant IrGST1 binds haemin in vitro

To further support evidence of haemin binding to the *Ir*GST1, crude extract from *E. coli* expressing *Ir*GST1 was incubated with haemin-agarose in a pull down assay. Roughly 75 % of *E. coli* extract proteins remained unbound in the supernatant, whereas the CDNB-specific activity was virtually lost (Fig. 5A), likely confined to the haemin-agarose pellet. After extensive washing with 20 mM phosphate buffer pH 7.4, 0.5 M NaCl, haemin-bound proteins were eluted with washing buffer supplemented with 1 M urea. SDS-PAGE analysis showed a major protein band of about 29 kDa (Fig. 5A), which was submitted to the peptide mass-fingerprint analysis that confirmed its identity as *Ir*GST1 with about 19% sequence coverage. To further elucidate the binding characteristics of haemin to *Ir*GST1, we evaluated the binding properties by spectrophotometry at visible wavelength range. Unbound haemin displays an absorption maximum at λ = 385 nm, but its absorption maximum undergoes intensifying red-shifts upon binding to *Ir*GST1, with isobestic point at λ = 402 nm, in the titration experiment where the *Ir*GST1 was treated as a ligand and haemin concentration was kept constant at 10 µM (Fig. 5B). The point of saturation on the monitoring wavelength (λ = 421 nm) was reached at 1:1 molar ratio (Fig. 5C), indicating that one *Ir*GST1 molecule binds one molecule of haemin.

3.6. Native IrGST1 is a haemin-binding dimer

In order to rule out a possible contribution of protein poly-histidine tag to haemin binding, untagged recombinant *Ir*GST1 was expressed in *E. coli* system and purified using two-step liquid chromatography by anion exchange chromatography (IEX) on the MonoQ column followed by size exclusion chromatography (SEC) on a Superdex 75 column (Fig. 6A). Monitoring absorbance at both λ = 280 nm and λ = 400 nm, revealed that the purified *Ir*GST1 already displayed some basal absorbance at 400 nm,

indicating that *Ir*GST1 strips endogenous haem from expressing *E. coli* cells (Fig. 6B). The molecular weight of the *Ir*GST1 was determined by SEC using calibration standards and calculated to be of 56.7 kDa implying a dimeric form (Fig. 6B). Isoelectric point of the native *Ir*GST1, determined experimentally by isoelectric focusing, was pI 5.5 (Supplemental Fig. S4). To assess the molecular arrangement of the *Ir*GST1 - haemin complex, the *Ir*GST1 was titrated with different molar concentrations of haemin and the products were analysed by SEC. As shown in the Fig. 6C, *Ir*GST1 has the capacity to bind haemin as a dimer. When haemin is in excess, up to eight to one molar ratios to *Ir*GST1, a fraction of the protein shifts towards higher molecular weights suggesting further polymerisation or aggregation of the *Ir*GST1-haemin complex (Supplementary Fig. S5).

4. Discussion

The glutathione S-transferases (GSTs) from pathogens that carry out disposal of toxic endogenous and exogenous compounds have been investigated as potential targets for development of efficient anti-parasitic drugs and vaccines for three decades (Brophy et al., 1990; Harwaldt et al., 2002; Nare et al., 1992; Ricciardi and Ndao, 2015; Wei et al., 2016; Zhan et al., 2005; Zhan et al., 2010).

In this work, we have characterised a novel haem-inducible GST from the hard tick *I. ricinus* (*Ir*GST1), which transcript was markedly up-regulated in blood-fed ticks compared to ticks fed with serum (Perner et al., 2016b). *Ir*GST1 belongs to the delta-/epsilon-class (insect type) GSTs and only one clear orthologue could be found among other 32 cytosolic GSTs identified in the genome of a closely relative species *I. scapularis* (Reddy et al., 2011). Accordingly, only one transcript orthologous to *Ir*GST1 could be found in transcriptomes available for other tick species. One haem-responsive GST, namely GST-19 (CE09995) has been identified using a proteomic approach among 36 nu-class members annotated in the genome of the model nematode *Caenorhabditis elegans* (Perally et al., 2008). Twenty six genes encoding GSTs were annotated in the mosquito *Aedes aegypti*¸ out of which the gene *gstx2* (new, unclassified class) showed an affinity for haematin (Lumjuan et al., 2007). Lately, a substantial up-regulation of this gene transcript was demonstrated using a transcriptome-wide analysis of haem influence on *A. aegypti* cell line (Bottino-Rojas et al., 2015).

Our phylogenetic analyses grouping haem-binding *Ir*GST1 with just one orthologue in each tick species (Fig. 1A, B) suggests that this tick-specific group likely exapted from an ancestral catalytic GST to form haem-binding GSTs under the evolution pressure exerted by their blood-feeding life style. This is supported by a distant phylogenetic positioning of tick putative haem-binding GSTs from other delta-/epsilon-class GSTs present in related non-haematophagous chelicerates (horseshoe crab and mites).

Several GSTs that have been at least partially characterised in ticks so far belong mostly to the mu-class (see (Shahein et al., 2013) for review). The first tick GST was purified from the larval stage of the cattle

tick *Rhipicephalus* (*Boophillus*) *microplus* using glutathione affinity chromatography (He et al., 1999). A gene encoding another mu-glass GST from *R. microplus* (referred to as as *Bm*GST) was isolated from salivary gland cDNA library, and its tissue and developmental stage profiling revealed that *bm-gst* gene is transcribed in salivary glands and midguts of the adult females but not in the larval stage (Rosa de Lima et al., 2002). The enzyme kinetic parameters of the recombinant *Bm*GST using the CDNB assay were determined together with the inhibitory potential for a number of compounds present in commercial acaricides (Vaz et al., 2004a). Two mu-class GSTs were cloned from the tick *Haemaphysalis longicornis* (*Hl*GST) and *Rhipicephalus appendiculatus* (*Ra*GST). The recombinant enzymes were reported to be effectively inhibited by acaricides, especially ethion and deltamethrin (Vaz et al., 2004b). Given the cross-reactivity of antibodies raised against recombinant *Hl*GST from *H. longicornis* with *Bm*GST from *R. microplus*, the cattle immunized with *Hl*GST were partially protected against infestation by the cattle ticks (Parizi et al., 2011) that implies tick GSTs as a candidate antigen for anti-tick vaccine development (de la Fuente et al., 2016). Most recently, the vaccination potential of *Hl*GST was tested against rabbit infestation with two closely related species *R. appendiculatus* and *R. sanquineus.* Despite the close similarity of GSTs from these tick species, the partial protection was obtained only against adult *R. appendiculatus* females (vaccine efficacy was reported to be of about 67%), but no protection was achieved against any stage of *R. sanquineus* (Sabadin et al., 2017). Another mu-class GST (tagged as *Ba*GST) was cloned from the Egyptian cattle tick *R.* (*B.*) *annulatus* and the active recombinant *Ba*GST was expressed and purified as fusion protein His-tagged protein (Shahein et al., 2008). This GST was later shown to be effectively inhibited by phenolic compounds and flavonoids from plant extracts but also by a haematin (Guneidy et al., 2014). RNAi-mediated silencing of the GST from *R. sanguineus* revealed the role of this enzyme in permethrin detoxification as the GST-KD ticks were more susceptible to the acaricide exposure (Duscher et al., 2014). The only partially characterised tick delta-/epsilon-class GST member was the *Dv*GST1 from *Dermacentor variabilis* (Fig. 1). The gene encoding *Dv*GST1 was reported to be specifically expressed in the tick gut and up-regulated by blood feeding (Dreher-Lesnick et al., 2006), which is suggestive to have a similar function as *Ir*GST1.

Ir-gst1 expression is tissue-specific for *I. ricinus* midgut (Perner et al., 2016b), where it is localised to the cytosol of the digest cell (Fig. 3B). Its mRNA and protein levels are markedly up-regulated by addition of a soluble heamin into the diet. The inducibility is more sensitive for soluble haemin rather than for haem bound as a prosthetic group of haemoglobin (Fig. 2). This might indicate that free haemin is taken up by the digest cells by an alternative route independently of the proposed haemoglobin-specific receptor mediated uptake, potentially disbalancing intracellular haem homeostasis (Lara et al., 2005; Sojka et al., 2013). Importantly, haem sensing in the tick midgut is independent of iron sensing in the tissue, as *Ir*GST1 expression is induced only by dietary haem, and not by dietary iron (Fig. 2D). Unlike the iron

homeostasis, which is controlled at the translational level by proteosynthesis of intracellular iron storage protein - ferritin 1 (Hajdušek et al., 2009; Kopacek et al., 2003; Perner et al., 2016a), haem-inducible expression of *Ir*GST1 is apparently controlled at the level of gene transcription. In mammals, inducible GSTs are known to be regulated through antioxidant response element by the Keap1-Nrf2 pathway (Kansanen et al., 2013). Although several Nrf2-related transcripts containing basic leucine zipper (bZIP) domain have been found to be present in the *I. ricinus* midgut transcriptome (Perner et al., 2016b), their possible role as haem-responsive transcription factor(s) remains to be investigated.

Beside the *ir-gst1* inducibility by a dietary haem, we found that the GSH-conjugation activity of recombinant *Ir*GST1 (determined by CDNB assay) is noncompetitively inhibited by soluble haemin but not by iron-free porphyrin ring (protoporhyrinogen IX) or protein-bound haem (myoglobin) (Fig. 4). We further showed that, in the native state, *Ir*GST1 forms a dimer and binds haem in an equimolar ratio. The Ki of haemin to *Ir*GST1 was in the mid nanomolar range, comparable to the inhibition constants reported earlier for GSTs from other hematophagous parasites (Torres-Rivera and Landa, 2008). Haem-binding properties were investigated for several nematode-specific nu-class GSTs from different hookworm species such as *Haemonchus contortus*, *Ancylostoma caninum*, *Necator americanus*, or *Ancylostoma ceylanicum* (van Rossum et al., 2004; Wei et al., 2016; Zhan et al., 2005; Zhan et al., 2010). Recombinant *Na*-GST1 from *N. americanus* elicited a significant reduction of hookworm burdens in vaccinated hamsters and hereby it became a leading vaccine candidate to prevent human hookworm infections (Zhan et al., 2010). Several haem-binding GSTs were also characterised in flatworms such as the sigma-class GSTs from flukes *Fasciola hepatica* (Brophy et al., 1990) or *Fg*GST-S1 from *F. gigantica* (Morphew et al., 2012). Much attention has been paid also to the haem-binding GSTs from different *Schistosoma* sp. (Walker et al., 1993) especially for their potential as promising vaccine candidates against human or bovine schistosomiasis (Capron et al., 2001; Capron et al., 1995; Ricciardi and Ndao, 2015). The most thoroughly investigated haem-binding GST has been *Pf*GST, the only cytosolic GST encoded in the genome of the malaria parasite *Plasmodium falciparum* (Harwaldt et al., 2002; Liebau et al., 2002). The quite abundant *Pf*GST, constituting about 3% of the total extractable proteins, forms in its native state a homodimer (Harwaldt et al., 2002) and was shown to capture haem that failed to be detoxified *via* polymerization in haemozoin (Liebau et al., 2002; Liebau et al., 2005). The 3D molecular structure of *Pf*GST was resolved by X-ray diffraction (Fritz-Wolf et al., 2003) that further allowed to perform a molecular docking for a variety of *Pf*GST ligands including haemin (Al-Qattan et al., 2016). We have demonstrated, using size exclusion chromatography (Fig. 6 C), that, in its native state, *Ir*GST1 binds haemin as a dimer at 1:1 molar ratio (Fig. 6 C). Moreover, the *in vitro* experiment showed that *Ir*GST1-haemin binding occurs in the absence of reduced glutathione, a feature reported also for the *Pf*GST (Liebau et al., 2009). In this work, the authors also described a transition of active *Pf*GST dimer to an

inactive tetramer. We have observed a similar polymerisation of *Ir*GST1 in the presence of molar excess of haemin (Supplementary Fig. S5), suggesting that inhibition of *Ir*GST1 enzyme activity by haemin resulted also in formation of inactive polymer.

As mentioned above, several GSTs became a potential target for development of anti-parasitic vaccines (Capron et al., 2001; Capron et al., 1995; Parizi et al., 2011; Ricciardi and Ndao, 2015; Zhan et al., 2010). Although *Ir*GST1 seems to be the only haem-binding GST expressed in the tick gut, its RNAi-mediated silencing did not result in any clear phenotype impairing tick feeding and further development. Also our pilot vaccination experiments with recombinant *Ir*GST1 did not elicit any protection of immunised rabbits against tick infestation (data not shown). These findings rather limit the potential of *Ir*GST1 as a target for anti-tick intervention.

Under normal situation, ticks seem to be capable to efficiently detoxify excessive haem *via* its aggregation in haemosomes (Lara et al., 2003). Based on the functional analogy with the *P. falciparum Pf*GST (Harwaldt et al., 2002; Liebau et al., 2009; Muller, 2015), our biochemical data indicates that *Ir*GST1 serves as a "back-up" guard molecule, i.e. by mopping up excess haemin and/or neutralising *via* lipid peroxidase activity the downstream consequence of haemin assault on membranes. Thus, *Ir*GST1 acts as ligandin, when high haemin levels override haemosome capacity and haemin is free in the cytosol and thus harmful to the tick.

Acknowledgements

This project was supported by the Czech Science Foundation-grant Nos. 13-11043S and 18-01832S to P.K., by the Czech Academy of Sciences MSM200961802 to J.P, and by the "Centre for research of pathogenicity and virulence of parasites" (No. CZ.02.1.01/0.0/0.0/16_019/0000759) funded by European Regional Development Fund (ERDF) and Ministry of Education, Youth and Sport (MEYS). The scientific stay of JP in the laboratory of PMB was supported by the project for student internationalisation and development IP 16-1807 from the University of South Bohemia. The authors gratefully acknowledge the assistance of Dr. Rebecca Stuart and Dr. Russ Morphew. We are also grateful to Jan Erhart for excellent technical support and Louise Robbertse for assistance with the graphical abstract.

References

Al-Qattan, M.N., Mordi, M.N., Mansor, S.M., 2016. Assembly of ligands interaction models for glutathione-S-transferases from *Plasmodium falciparum*, human and mouse using enzyme kinetics and molecular docking. Comput Biol Chem 64, 237-249.

Atkinson, H.J., Babbitt, P.C., 2009. Glutathione transferases are structural and functional outliers in the thioredoxin fold. Biochemistry 48, 11108-11116.

Awasthi, Y.C., Yang, Y., Tiwari, N.K., Patrick, B., Sharma, A., Li, J., Awasthi, S., 2004. Regulation of 4-hydroxynonenal-mediated signaling by glutathione S-transferases. Free Radic Biol Med 37, 607-619.

Bottino-Rojas, V., Talyuli, O.A., Jupatanakul, N., Sim, S., Dimopoulos, G., Venancio, T.M., Bahia, A.C., Sorgine, M.H., Oliveira, P.L., Paiva-Silva, G.O., 2015. Heme Signaling Impacts Global Gene Expression, Immunity and Dengue Virus Infectivity in *Aedes aegypti*. PLoS One 10, e0135985.

Brophy, P.M., Southan, C., Barrett, J., 1989. Glutathione transferases in the tapeworm *Moniezia expansa*. Biochem J 262, 939-946.

Brophy, P.M., Crowley, P., Barrett, J., 1990. Detoxification reactions of *Fasciola hepatica* cytosolic glutathione transferases. Molecular and biochemical parasitology 39, 155-161.

Capron, A., Riveau, G., Grzych, J.M., Boulanger, D., Capron, M., Pierce, R., 1995. Development of a vaccine strategy against human and bovine schistosomiasis. Background and update. Mem Inst Oswaldo Cruz 90, 235-240.

Capron, A., Capron, M., Dombrowicz, D., Riveau, G., 2001. Vaccine strategies against schistosomiasis: from concepts to clinical trials. Int Arch Allergy Immunol 124, 9-15.

Cheng, J.Z., Sharma, R., Yang, Y., Singhal, S.S., Sharma, A., Saini, M.K., Singh, S.V., Zimniak, P., Awasthi, S., Awasthi, Y.C., 2001. Accelerated metabolism and exclusion of 4-hydroxynonenal through induction of RLIP76 and hGST5.8 is an early adaptive response of cells to heat and oxidative stress. J Biol Chem 276, 41213-41223.

de la Fuente, J., Estrada-Pena, A., Venzal, J.M., Kocan, K.M., Sonenshine, D.E., 2008. Overview: Ticks as vectors of pathogens that cause disease in humans and animals. Front Biosci 13, 6938-6946.

de la Fuente, J., Kopacek, P., Lew-Tabor, A., Maritz-Olivier, C., 2016. Strategies for new and improved vaccines against ticks and tick-borne diseases. Parasite Immunol 38, 754-769.

Dreher-Lesnick, S.M., Mulenga, A., Simser, J.A., Azad, A.F., 2006. Differential expression of two glutathione S-transferases identified from the American dog tick, *Dermacentor variabilis*. Insect Molecular Biology 15, 445-453.

Duscher, G.G., Galindo, R.C., Tichy, A., Hummel, K., Kocan, K.M., de la Fuente, J., 2014. Glutathione S-transferase affects permethrin detoxification in the brown dog tick, *Rhipicephalus sanguineus*. Ticks Tick Borne Dis 5, 225-233.

Enayati, A.A., Ranson, H., Hemingway, J., 2005. Insect glutathione transferases and insecticide resistance. Insect Molecular Biology 14, 3-8.

Franta, Z., Frantova, H., Konvickova, J., Horn, M., Sojka, D., Mares, M., Kopacek, P., 2010. Dynamics of digestive proteolytic system during blood feeding of the hard tick *Ixodes ricinus*. Parasit Vectors 3, 119.

Fritz-Wolf, K., Becker, A., Rahlfs, S., Harwaldt, P., Schirmer, R.H., Kabsch, W., Becker, K., 2003. X-ray structure of glutathione S-transferase from the malarial parasite *Plasmodium falciparum*. Proc Natl Acad Sci U S A 100, 13821-13826.

Graca-Souza, A.V., Maya-Monteiro, C., Paiva-Silva, G.O., Braz, G.R., Paes, M.C., Sorgine, M.H., Oliveira, M.F., Oliveira, P.L., 2006. Adaptations against heme toxicity in blood-feeding arthropods. Insect Biochem Mol Biol 36, 322-335.

552 Grunclova, L., Horn, M., Vancova, M., Sojka, D., Franta, Z., Mares, M., Kopacek, P., 2006. Two secreted
553 cystatins of the soft tick *Ornithodoros moubata*: differential expression pattern and inhibitory
554 specificity. Biological Chemistry 387, 1635-1644.
555 Gulia-Nuss, M., Nuss, A.B., Meyer, J.M., Sonenshine, D.E., Roe, R.M., Waterhouse, R.M., Sattelle, D.B., de
556 la Fuente, J., Ribeiro, J.M., Megy, K., Thimmapuram, J., Miller, J.R., Walenz, B.P., Koren, S., Hostetler,
557 J.B., Thiagarajan, M., Joardar, V.S., Hannick, L.I., Bidwell, S., Hammond, M.P., Young, S., Zeng, Q.,
558 Abrudan, J.L., Almeida, F.C., Ayllon, N., Bhide, K., Bissinger, B.W., Bonzon-Kulichenko, E.,
559 Buckingham, S.D., Caffrey, D.R., Caimano, M.J., Croset, V., Driscoll, T., Gilbert, D., Gillespie, J.J.,
560 Giraldo-Calderon, G.I., Grabowski, J.M., Jiang, D., Khalil, S.M., Kim, D., Kocan, K.M., Koci, J., Kuhn,
561 R.J., Kurtti, T.J., Lees, K., Lang, E.G., Kennedy, R.C., Kwon, H., Perera, R., Qi, Y., Radolf, J.D.,
562 Sakamoto, J.M., Sanchez-Gracia, A., Severo, M.S., Silverman, N., Simo, L., Tojo, M., Tornador, C., Van
563 Zee, J.P., Vazquez, J., Vieira, F.G., Villar, M., Wespiser, A.R., Yang, Y., Zhu, J., Arensburger, P.,
564 Pietrantonio, P.V., Barker, S.C., Shao, R., Zdobnov, E.M., Hauser, F., Grimmelikhuijzen, C.J., Park, Y.,
565 Rozas, J., Benton, R., Pedra, J.H., Nelson, D.R., Unger, M.F., Tubio, J.M., Tu, Z., Robertson, H.M.,
566 Shumway, M., Sutton, G., Wortman, J.R., Lawson, D., Wikel, S.K., Nene, V.M., Fraser, C.M., Collins,
567 F.H., Birren, B., Nelson, K.E., Caler, E., Hill, C.A., 2016. Genomic insights into the *Ixodes scapularis*
568 tick vector of Lyme disease. Nat Commun 7, 10507.
569 Guneidy, R.A., Shahein, Y.E., Abouelella, A.M., Zaki, E.R., Hamed, R.R., 2014. Inhibition of the
570 recombinant cattle tick *Rhipicephalus* (*Boophilus*) *annulatus* glutathione S-transferase. Ticks Tick
571 Borne Dis 5, 528-536.
572 Habig, W.H., Pabst, M.J., Fleischner, G., Gatmaitan, Z., Arias, I.M., Jakoby, W.B., 1974. The identity of
573 glutathione S-transferase B with ligandin, a major binding protein of liver. Proceedings of the
574 National Academy of Sciences 71, 3879-3882.
575 Hajdušek, O., Sojka, D., Kopáček, P., Burešová, V., Franta, Z., Šauman, I., Winzerling, J., Grubhoffer, L.,
576 2009. Knockdown of proteins involved in iron metabolism limits tick reproduction and development.
577 Proceedings of the National Academy of Sciences 106, 1033-1038.
578 Harwaldt, P., Rahlfs, S., Becker, K., 2002. Glutathione S-transferase of the malarial parasite *Plasmodium*
579 *falciparum*: Characterization of a potential drug target. Biological Chemistry 383, 821-830.
580 He, H., Chen, A.C., Davey, R.B., Ivie, G.W., George, J.E., 1999. Characterization and molecular cloning of a
581 glutathione S-transferase gene from the tick, *Boophilus microplus* (Acari: Ixodidae). Insect Biochem
582 Mol Biol 29, 737-743.
583 Jaffe, J.J., Lambert, R.A., 1986. Glutathione S-transferase in adult *Dirofilaria immitis* and *Brugia pahangi*.
584 Molecular and biochemical parasitology 20, 199-206.
585 Kansanen, E., Kuosmanen, S.M., Leinonen, H., Levonen, A.L., 2013. The Keap1-Nrf2 pathway:
586 Mechanisms of activation and dysregulation in cancer. Redox Biol 1, 45-49.
587 Katoh, K., Misawa, K., Kuma, K., Miyata, T., 2002. MAFFT: a novel method for rapid multiple sequence
588 alignment based on fast Fourier transform. Nucleic Acids Res 30, 3059-3066.
589 Kearse, M., Moir, R., Wilson, A., Stones-Havas, S., Cheung, M., Sturrock, S., Buxton, S., Cooper, A.,
590 Markowitz, S., Duran, C., Thierer, T., Ashton, B., Meintjes, P., Drummond, A., 2012. Geneious Basic:
591 An integrated and extendable desktop software platform for the organization and analysis of
592 sequence data. Bioinformatics 28, 1647-1649.
593 Kopacek, P., Zdychova, J., Yoshiga, T., Weise, C., Rudenko, N., Law, J.H., 2003. Molecular cloning,
594 expression and isolation of ferritins from two tick species--*Ornithodoros moubata* and *Ixodes ricinus*.
595 Insect Biochem Mol Biol 33, 103-113.
596 Kröber, T., Guerin, P.M., 2007. *In vitro* feeding assays for hard ticks. Trends in Parasitology 23, 445-449.
597 Lara, F.A., Lins, U., Paiva-Silva, G., Almeida, I.C., Braga, C.M., Miguens, F.C., Oliveira, P.L., Dansa-Petretski,
598 M., 2003. A new intracellular pathway of haem detoxification in the midgut of the cattle tick

Boophilus microplus: aggregation inside a specialized organelle, the hemosome. J Exp Biol 206, 1707-1715.

Lara, F.A., Lins, U., Bechara, G.H., Oliveira, P.L., 2005. Tracing heme in a living cell: hemoglobin degradation and heme traffic in digest cells of the cattle tick *Boophilus microplus*. J Exp Biol 208, 3093-3101.

Lara, F.A., Pohl, P.C., Gandara, A.C., Ferreira, J.d.S., Nascimento-Silva, M.C., Bechara, G.H., Sorgine, M.H.F., Almeida, I.C., Vaz, I.d.S., Oliveira, P.L., 2015. ATP Binding Cassette Transporter Mediates Both Heme and Pesticide Detoxification in Tick Midgut Cells. PLoS One 10, e0134779.

Liebau, E., Bergmann, B., Campbell, A.M., Teesdale-Spittle, P., Brophy, P.M., Luersen, K., Walter, R.D., 2002. The glutathione S-transferase from *Plasmodium falciparum*. Molecular and biochemical parasitology 124, 85-90.

Liebau, E., De Maria, F., Burmeister, C., Perbandt, M., Turella, P., Antonini, G., Federici, G., Giansanti, F., Stella, L., Lo Bello, M., Caccuri, A.M., Ricci, G., 2005. Cooperativity and pseudo-cooperativity in the glutathione S-transferase from *Plasmodium falciparum*. J Biol Chem 280, 26121-26128.

Liebau, E., Dawood, K.F., Fabrini, R., Fischer-Riepe, L., Perbandt, M., Stella, L., Pedersen, J.Z., Bocedi, A., Petrarca, P., Federici, G., Ricci, G., 2009. Tetramerization and cooperativity in *Plasmodium falciparum* glutathione S-transferase are mediated by atypic loop 113-119. J Biol Chem 284, 22133-22139.

Lumjuan, N., Stevenson, B.J., Prapanthadara, L.A., Somboon, P., Brophy, P.M., Loftus, B.J., Severson, D.W., Ranson, H., 2007. The *Aedes aegypti* glutathione transferase family. Insect Biochem Mol Biol 37, 1026-1035.

Mashiyama, S.T., Malabanan, M.M., Akiva, E., Bhosle, R., Branch, M.C., Hillerich, B., Jagessar, K., Kim, J., Patskovsky, Y., Seidel, R.D., Stead, M., Toro, R., Vetting, M.W., Almo, S.C., Armstrong, R.N., Babbitt, P.C., 2014. Large-Scale Determination of Sequence, Structure, and Function Relationships in Cytosolic Glutathione Transferases across the Biosphere. Plos Biology 12.

Morphew, R.M., Eccleston, N., Wilkinson, T.J., McGarry, J., Perally, S., Prescott, M., Ward, D., Williams, D., Raman, S.P.M., Ravikumar, G., Saifullah, M.K., Abidi, S.M.A., McVeigh, P., Maule, A.G., Brophy, P.M., LaCourse, E.J., 2012. Proteomics and in Silico Approaches To Extend Understanding of the Glutathione Transferase Superfamily of the Tropical Liver Fluke *Fasciola gigantica*. Journal of Proteome Research 11, 5876-5889.

Morphew, R.M., MacKintosh, N., Harta, E.H., Prescott, M., LaCoursec, E.J., Brophy, P.M., 2014. In vitro biomarker discovery in the parasitic flatworm *Fasciola hepatica* for monitoring chemotherapeutic treatment. EuPA Open Proteomics 3, 85-99.

Muller, S., 2015. Role and Regulation of Glutathione Metabolism in *Plasmodium falciparum*. Molecules 20, 10511-10534.

Nare, B., Smith, J.M., Prichard, R.K., 1992. Mechanisms of inactivation of *Schistosoma mansoni* and mammalian glutathione S-transferase activity by the antischistosomal drug oltipraz. Biochemical Pharmacology 43, 1345-1351.

Parizi, L.F., Utiumi, K.U., Imamura, S., Onuma, M., Ohashi, K., Masuda, A., Vaz, I.D., 2011. Cross immunity with *Haemaphysalis longicornis* glutathione S-transferase reduces an experimental *Rhipicephalus* (*Boophilus*) *microplus* infestation. Experimental Parasitology 127, 113-118.

Perally, S., Lacourse, E.J., Campbell, A.M., Brophy, P.M., 2008. Heme transport and detoxification in nematodes: subproteomics evidence of differential role of glutathione transferases. Journal of Proteome Research 7, 4557-4565.

Perner, J., Sobotka, R., Šíma, R., Konvičková, J., Sojka, D., Oliveira, P.L.d., Hajdušek, O., Kopáček, P., 2016a. Acquisition of exogenous haem is essential for tick reproduction. eLife 5, e12318.

Perner, J., Provazník, J., Schrenková, J., Urbanová, V., Ribeiro, J.M.C., Kopáček, P., 2016b. RNA-seq analyses of the midgut from blood- and serum-fed *Ixodes ricinus* ticks. Scientific Reports 6, 36695.

Pfaffl, M.W., 2001. A new mathematical model for relative quantification in real-time RT-PCR. Nucleic Acids Res 29, e45.

Reddy, B.P., Prasad, G.B., Raghavendra, K., 2011. In silico analysis of glutathione S-transferase supergene family revealed hitherto unreported insect specific delta- and epsilon-GSTs and mammalian specific mu-GSTs in *Ixodes scapularis* (Acari: Ixodidae). Comput Biol Chem 35, 114-120.

Ricciardi, A., Ndao, M., 2015. Still hope for schistosomiasis vaccine. Hum Vaccin Immunother 11, 2504-2508.

Ronquist, F., Huelsenbeck, J.P., 2003. MrBayes 3: Bayesian phylogenetic inference under mixed models. Bioinformatics 19, 1572-1574.

Rosa de Lima, M.F., Sanchez Ferreira, C.A., Joaquim de Freitas, D.R., Valenzuela, J.G., Masuda, A., 2002. Cloning and partial characterization of a *Boophilus microplus* (Acari: Ixodidae) glutathione S-transferase. Insect Biochem Mol Biol 32, 747-754.

Sabadin, G.A., Parizi, L.F., Kiio, I., Xavier, M.A., da Silva Matos, R., Camargo-Mathias, M.I., Githaka, N.W., Nene, V., da Silva Vaz, I., Jr., 2017. Effect of recombinant glutathione S-transferase as vaccine antigen against *Rhipicephalus appendiculatus* and *Rhipicephalus sanguineus* infestation. Vaccine 35, 6649-6656.

Shahein, Y., Abouelella, A., Hamed, R., 2013. Glutathione S-Transferase Genes from Ticks, in: Baptista, G.R. (Ed.), An Integrated View of the Molecular Recognition and Toxinology - From Analytical Procedures to Biomedical Applications. InTECH Open, pp. 267-289.

Shahein, Y.E., El Sayed El-Hakim, A., Abouelella, A.M., Hamed, R.R., Allam, S.A., Farid, N.M., 2008. Molecular cloning, expression and characterization of a functional GSTmu class from the cattle tick *Boophilus annulatus*. Vet Parasitol 152, 116-126.

Sojka, D., Franta, Z., Horn, M., Caffrey, C.R., Mareš, M., Kopáček, P., 2013. New insights into the machinery of blood digestion by ticks. Trends in Parasitology 29, 276-285.

Sonenshine, D.E., Roe, R.M., 2014. Biology of ticks, 2 ed. Oxford University Press.

Stamatakis, A., 2006. RAxML-VI-HPC: Maximum likelihood-based phylogenetic analyses with thousands of taxa and mixed models. Bioinformatics 22, 2688-2690.

Swofford, D.L., 2003. Phylogenetic Analysis Using Parsimony (*and Other Methods). Version 4. . Sinauer Associates, Sunderland, Massachusetts.

Torres-Rivera, A., Landa, A., 2008. Glutathione transferases from parasites: a biochemical view. Acta Trop 105, 99-112.

Townsend, D.M., Tew, K.D., 2003. The role of glutathione-S-transferase in anti-cancer drug resistance. Oncogene 22, 7369-7375.

van Rossum, A.J., Jefferies, J.R., Rijsewijk, F.A.M., LaCourse, E.J., Teesdale-Spittle, P., Barrett, J., Tait, A., Brophy, P.M., 2004. Binding of Hematin by a New Class of Glutathione Transferase from the Blood-Feeding Parasitic Nematode *Haemonchus contortus*. Infection and Immunity 72, 2780-2790.

Vaz, I.D., Lermen, T.T., Michelon, A., Ferreira, C.A.S., de Freitas, D.R.J., Termignoni, C., Masuda, A., 2004a. Effect of acaricides on the activity of a *Boophilus microplus* glutathione S-transferase. Vet Parasitol 119, 237-245.

Vaz, I.D., Imamura, S., Ohashi, K., Onuma, M., 2004b. Cloning, expression and partial characterization of a *Haemaphysalis longicornis* and a *Rhipicephalus appendiculatus* glutathione S-transferase. Insect Molecular Biology 13, 329-335.

Walker, J., Crowley, P., Moreman, A.D., Barrett, J., 1993. Biochemical properties of cloned glutathione S-transferases from *Schistosoma mansoni* and *Schistosoma japonicum*. Mol Biochem Parasitol 61, 255-264.

Wei, J., Damania, A., Gao, X., Liu, Z., Mejia, R., Mitreva, M., Strych, U., Bottazzi, M.E., Hotez, P.J., Zhan, B., 2016. The hookworm *Ancylostoma ceylanicum* intestinal transcriptome provides a platform for selecting drug and vaccine candidates. Parasit Vectors 9.

Wilce, M.C.J., Parker, M.W., 1994. Structure and Function of Glutathione S-Transferases. Biochimica Et Biophysica Acta-Protein Structure and Molecular Enzymology 1205, 1-18.

Zhan, B., Liu, S., Perally, S., Xue, J., Fujiwara, R., Brophy, P., Xiao, S., Liu, Y., Feng, J., Williamson, A., Wang, Y., Bueno, L.L., Mendez, S., Goud, G., Bethony, J.M., Hawdon, J.M., Loukas, A., Jones, K., Hotez, P.J., 2005. Biochemical Characterization and Vaccine Potential of a Heme-Binding Glutathione Transferase from the Adult Hookworm *Ancylostoma caninum*. Infection and Immunity 73, 6903-6911.

Zhan, B., Perally, S., Brophy, P.M., Xue, J., Goud, G., Liu, S., Deumic, V., de Oliveira, L.M., Bethony, J., Bottazzi, M.E., Jiang, D., Gillespie, P., Xiao, S.h., Gupta, R., Loukas, A., Ranjit, N., Lustigman, S., Oksov, Y., Hotez, P., 2010. Molecular Cloning, Biochemical Characterization, and Partial Protective Immunity of the Heme-Binding Glutathione S-Transferases from the Human Hookworm *Necator americanus*. Infection and Immunity 78, 1552-1563.

Legends to the Figures

Fig 1. Phylogeny and multiple alignment of selected chelicerate delta-/epsilon-class GST homologues. (A) Maximum likelihood phylogenetic tree of delta-/epsilon-class GST homologues in chelicerates with *Ir*GST1and its tick orthologues grouping in one well-supported clade. Nodal supports are shown for maximum likelihood and maximum parsimony bootstraps and Bayesian inference posterior probability. Sequences used for multiple amino-acid alignment in Fig. 1B are shown in bold **(B)** Multiple amino-acid alignment of *Ir*GST1 sequence with putative orthologues from other ticks and selected delta-/epsilon-class GSTs from other chelicerates. **Hard ticks**: *I. ricinus* - *Ir*GST1 (this work, GenBank MF984398); *I. scapularis* – *Is*GSTD2 (GenBank XM_002436245); *I. persulcatus* (GenBank GBXQ01020781); *R. appendiculatus* (GenBank GEDV01003209); *R. microplus* (GenBank GEFA01011362); *A. aureolatum* (GenBank GFAC01002707); *D. variabilis Dv*GST1 (GenBank AY241958). **Soft ticks**: *O. moubata* (GenBank GFJQ02000585); *C. mimon* (GenBank GEIB01001162). **Mites**: *D. gallinae* (GenBank KR337506); *G. occidentalis* (GenBank XM_003746739); *T. urticae* (GenBank XM_015936065); *S. scabiei* (GenBank AY649788); *V. destructor* (GenBank XP_022657236). **Horseshoe crab**: *L. polyphemus* (GenBank XM_013931267). The hash symbol points to the conserved tyrosine residue of Y-type GSTs. The asterisks and dashed red frame depict the conserved GSTs signature motif of *Ir*GST1 orthologues as SRAI(A/G). The column next to the sequences shows sequence identity percentage related to *Ir*GST1.

Fig. 2. Analysis of *ir-gst1* expression by RT-qPCR and *Ir*GST1 levels by Western blotting. (A, B) Analysis of midguts of ticks fed serum for 5 days (S), serum supplemented with haemin solvent (S-mock), 625 μM haemin (S+hm), 1% haemoglobin (equimolar to 625 μM haemin) (S+Hb), or reconstituted blood

with 50% haematocrit (whole blood, WB). **(A)** RT-qPCR expression data are normalised against *elongation factor 1α* (*ef1α*). Shown data represent mean and SEM from three biological replicates. **(B)** Tick midgut homogenates were separated using reducing SDS-PAGE. Western Blot analysis was performed using specific rabbit anti-serum raised against *Ir*GST1 (α*Ir*GST1) diluted 1:5000. **(C)** Midgut homogenates of ticks fed, for five days, serum supplemented with increasing haemin concentration were separated on reducing SDS-PAGE and Western Blot analysis was performed using α*Ir*GST1 (1:5000). **(D)** Midgut homogenates of seven days fed ticks, five days fed serum and for two consecutive days fed serum supplemented with 3 mg/ml bovine holo-Transferrin (Tf) or 10 mg/ml bovine Haemoglobin (Hb), were separated on reducing SDS-PAGE and Western Blot analysis was performed using α*Ir*GST1 (1:5000) and α*Ir*Fer1 (1:50)

Fig. 3. RNAi verification and phenotypisation. Adult *I. ricinus* ticks were injected with *ir-gst1* or *gfp* (control) dsRNA and allowed to recover for 24 hours (Day 0). Ticks (n = 25) were then placed on a rabbit and allowed to feed naturally for indicated time-points (Day 3, Day 5, and Day 7), then forcibly removed, weighed out, and their midguts dissected ($n \geq 3$). The remaining ticks were allowed to feed until repletion. **(A)** Tick midgut homogenates were separated by reducing SDS-PAGE and *Ir*GST1 protein levels were analysed by Western blotting using α*Ir*GST1 antibody (1:5000). **(B)** Sections were prepared from guts dissected from semi-engorged *I. ricinus* females (5 days of feeding). Section were labelled with α*Ir*GST1 serum (1:100) and Alexa488-conjugated anti-mouse antibody (left). DAPI was used to counterstain the nuclei. Sections were also stained with toluidine blue (right) - general structure of the tick gut showing the boundary between the gut epithelium and the gut lumen, containing large haemoglobin crystals (Hb) and developed digest gut cells (dGC); Nc - nuclei. **(C)** Column graph of tick weights before feeding and from individual time-points of feeding. Mean and SEM are shown, $n \geq 3$. **(D)** Oviposition and larvae hatching from fully engorged females upon RNAi.

Fig. 4. Purification of recombinant *Ir*GST1, substrate profiling, and haemin inhibition assay. (A) Soluble recombinant $(His)_6$-tagged *Ir*GST1 was purified from the lysate of expressing *E. coli* using Ni^{2+}-IMAC under native conditions and fractions were analysed by reducing SDS-PAGE. Crude – *E. coli* lysate; Flow-through – unbound proteins; Elution – *Ir*GST1 eluted with 200 mM imidazole. **(B)** *Ir*GST1 from *I. ricinus* was tested for specific activities in spectrophotometric assays using GST model substrates; recombinant GST from *Fasciola gigantica* was used as a positive control (Morphew et al., 2012); 1-chloro-2,4-dinitrobenzene (CDNB) was used to test GSH-conjugation activity, trans 2-nonenal (T2N) was used to test GST-mediated reactions with reactive carbonyls, cumene hydroperoxide (C-HPx) was used to test peroxidase activity **(C)** Inhibition assays of haemin on CDNB activity of *Ir*GST1 and *F. gigantica*

765 over a range of different CDNB concentrations. **(D)** Dixon plot of inhibitory properties of haemin on
766 *Ir*GST1 activity under different substrate (CDNB) concentrations. Calculated inhibitory constant (Ki) is
767 shown. **(E)** CDNB assays testing inhibitory properties of haemin, haematin, protoporphyrin IX (PPIX),
768 and myoglobin in a dilution series. **(B, D, E)** Mean and SEM from three independent measurements are
769 shown.
770

771 **Fig. 5. Assessment of haemin binding to *Ir*GST1 by haemin-agarose pull down and by VIS-**
772 **spectrophotometry (A)** SDS-PAGE of the crude *E. coli* homogenate fractionated by haemin-agarose
773 affinity absorption. Induced homogenate of *E. coli* expressing *Ir*GST1 was subjected to affinity pull-down
774 by incubating the homogenate with haemin-agarose beads. Red asterisk indicates the protein band eluted
775 with 1 M urea and submitted for mass-fingerprint identification. CDNB activities (nmol CDNB/min/mg
776 protein) of individual fractions are shown below the gel picture, mean ± SEM from three measurements.
777 Activity of eluted fraction was not determined due to the presence denaturating urea in elution buffer. **(B)**
778 Titration of *Ir*GST1 was carried out in a range of molar ratios to the constant concentration of 10 μM
779 haemin. **(C)** A plot of absorbance values at 421 nm in relation to molar ratios of *Ir*GST1 and haemin.
780

781 **Fig. 6. Purification and haem-binding of untagged *Ir*GST1. (A)** SDS-PAGE monitoring a two-step
782 purification of untagged *Ir*GST1 from *E. coli* homogenate (Crude). First step was performed by anion
783 exchange (IEX) chromatography using MonoQ column. Second step was performed by size-exclusion
784 chromatography (SEC) using Superdex 75 column. **(B)** SEC chromatogram of purified untagged *Ir*GST1
785 detected at 280 (black line) and 400 nm (red line). The elution volumes of molecular weight standards are
786 indicated by arrows. The deduced molecular weight of *Ir*GST1 was calculated using a logarithmic
787 standard curve. **(C)** SEC chromatogram detecting both 280 nm (black line) and 400 nm (red lines) of
788 purified *Ir*GST1 pre-incubated with varying molar ratios of haemin.
789

790 **Legends to the Supplementary Figures**
791

792 **Supplementary Fig. S1. Multiple amino acid alignment of *Ir*GST1 sequence with putative**
793 **homologues of delta-/epsilon-class GSTs from *I.scapularis* genome.** *Ir*GST1 (*Ixodes ricinus*, this work,
794 GenBank MF984398); Right panel table – Nomenclature, VectorBase and GenBank accession Nos of *I.*
795 *scapularis* genes encoding delta-/epsilon-class GSTs adopted from (Reddy et al., 2011).
796

797 **Supplementary Fig. S2. Immunohistochemistry evaluation of lipid peroxidation.** Sections were
798 prepared from guts dissected from semi-engorged *I. ricinus* females (5 days of feeding). Section were

799 labelled with rabbit α4-HNE (1:300) and Alexa488-conjugated anti-rabbit antibody (left). DAPI was used
800 a counterstain. Sections were also stained with toluidine blue (right) - general structure of the tick gut
801 showing the boundary between the gut epithelium and the gut lumen, containing large haemoglobin
802 crystals (Hb) and digest gut cells (dGC); Nc - nuclei.
803
804 **Supplementary Fig. S3. Binding of *Ir*GST1 to glutathione or S-hexyl glutathione agarose. (A)**
805 Activity measurements with titrated 1-chloro-2,4-dinitrobenzene (CDNB) concentrations to calculate
806 Michaelis-Menten constant (Km). **(B)** Activity measurements with titrated glutathione (GSH)
807 concentrations to calculate Michaelis-Menten constant (Km). **(C)** Induced *E. coli* fraction as well as Ni^{2+}-
808 IMAC purified *Ir*GST1 were subjected to glutathione or S-hexyl glutathione (S6) agarose. Individual
809 fractions were examined by SDS-PAGE and activity measurements. Mean and SEM are shown, n = 3. FT
810 - flow-through, E - elution, N.D. - not determined with a given detection limit.
811
812 **Supplementary Fig. S4. Isoelectric focusing electrophoresis of purified untagged *Ir*GST1.** Standard
813 pI values of the markers (M) are indicated on the left.
814
815 **Supplementary Fig. S5. Haem-binding size exclusion chromatography (SEC).** SEC chromatogram
816 detecting both 280 and 400 nm of purified untagged *Ir*GST1 pre-incubated with varying molar ratios of
817 haemin. Arrows point towards a deduced dimeric form of the protein, asterisks denote a higher molecular
818 weight *Ir*GST1:haemin complex as a potential polymer.

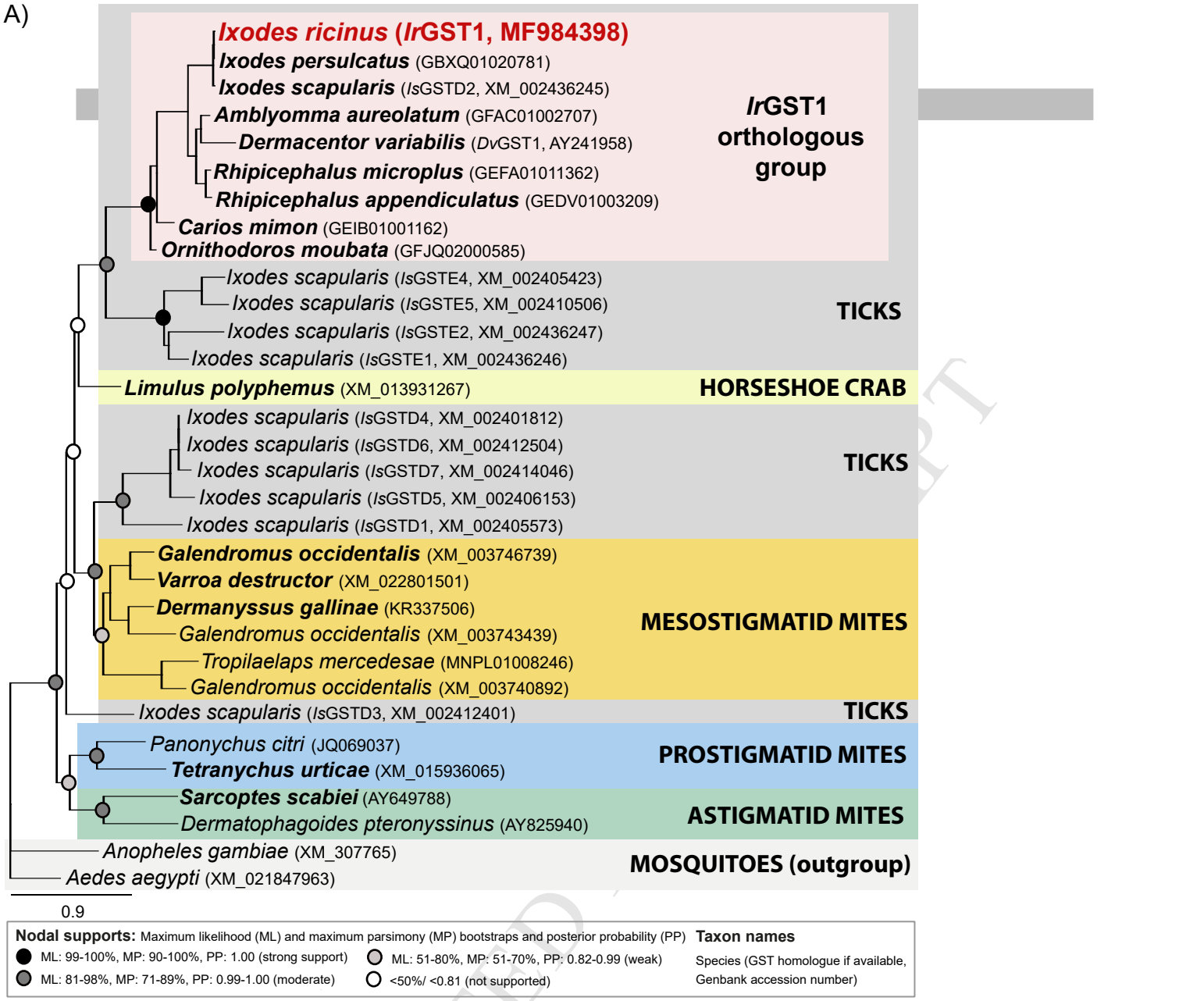
A)
Ixodes ricinus (IrGST1, MF984398)
Ixodes persulcatus (GBXQ01020781)
Ixodes scapularis (IsGSTD2, XM_002436245)
Amblyomma aureolatum (GFAC01002707)
Dermacentor variabilis (DvGST1, AY241958)
Rhipicephalus microplus (GEFA01011362)
Rhipicephalus appendiculatus (GEDV01003209)
Carios mimon (GEIB01001162)
Ornithodoros moubata (GFJQ02000585)
IrGST1 orthologous group
Ixodes scapularis (IsGSTE4, XM_002405423)
Ixodes scapularis (IsGSTE5, XM_002410506)
Ixodes scapularis (IsGSTE2, XM_002436247)
Ixodes scapularis (IsGSTE1, XM_002436246)
TICKS
Limulus polyphemus (XM_013931267)
HORSESHOE CRAB
Ixodes scapularis (IsGSTD4, XM_002401812)
Ixodes scapularis (IsGSTD6, XM_002412504)
Ixodes scapularis (IsGSTD7, XM_002414046)
Ixodes scapularis (IsGSTD5, XM_002406153)
Ixodes scapularis (IsGSTD1, XM_002405573)
TICKS
Galendromus occidentalis (XM_003746739)
Varroa destructor (XM_022801501)
Dermanyssus gallinae (KR337506)
Galendromus occidentalis (XM_003743439)
Tropilaelaps mercedesae (MNPL01008246)
Galendromus occidentalis (XM_003740892)
MESOSTIGMATID MITES
Ixodes scapularis (IsGSTD3, XM_002412401)
TICKS
Panonychus citri (JQ069037)
Tetranychus urticae (XM_015936065)
PROSTIGMATID MITES
Sarcoptes scabiei (AY649788)
Dermatophagoides pteronyssinus (AY825940)
ASTIGMATID MITES
Anopheles gambiae (XM_307765)
Aedes aegypti (XM_021847963)
MOSQUITOES (outgroup)
0.9
Nodal supports: Maximum likelihood (ML) and maximum parsimony (MP) bootstraps and posterior probability (PP)
ML: 99-100%, MP: 90-100%, PP: 1.00 (strong support)
ML: 81-98%, MP: 71-89%, PP: 0.99-1.00 (moderate)
ML: 51-80%, MP: 51-70%, PP: 0.82-0.99 (weak)
<50%/ <0.81 (not supported)
Taxon names
Species (GST homologue if available, Genbank accession number)

B)

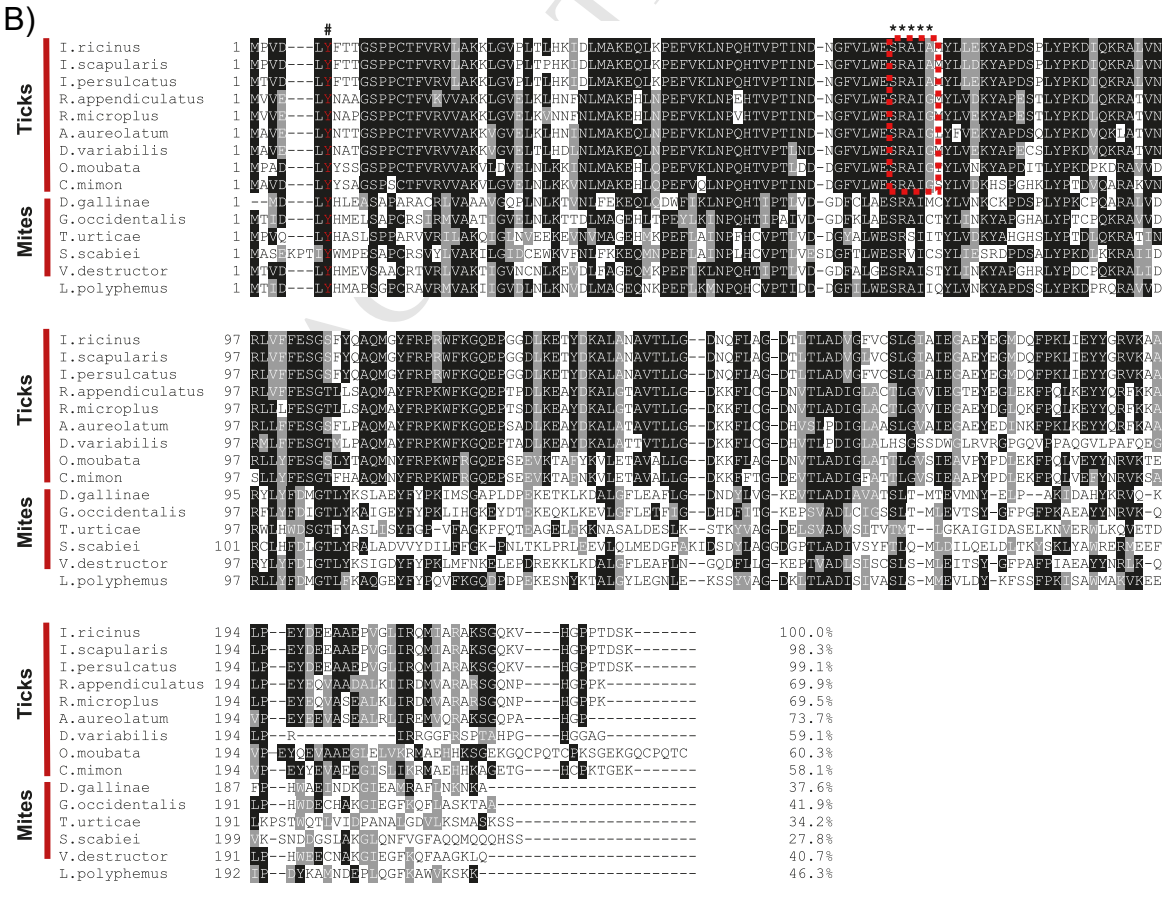
Ticks
Mites
I.ricinus
I.scapularis
I.persulcatus
R.appendiculatus
R.microplus
A.aureolatum
D.variabilis
O.moubata
C.mimon
D.gallinae
G.occidentalis
T.urticae
S.scabiei
V.destructor
L.polyphemus
100.0%
98.3%
99.1%
69.9%
69.5%
73.7%
59.1%
60.3%
58.1%
37.6%
41.9%
34.2%
27.8%
40.7%
46.3%

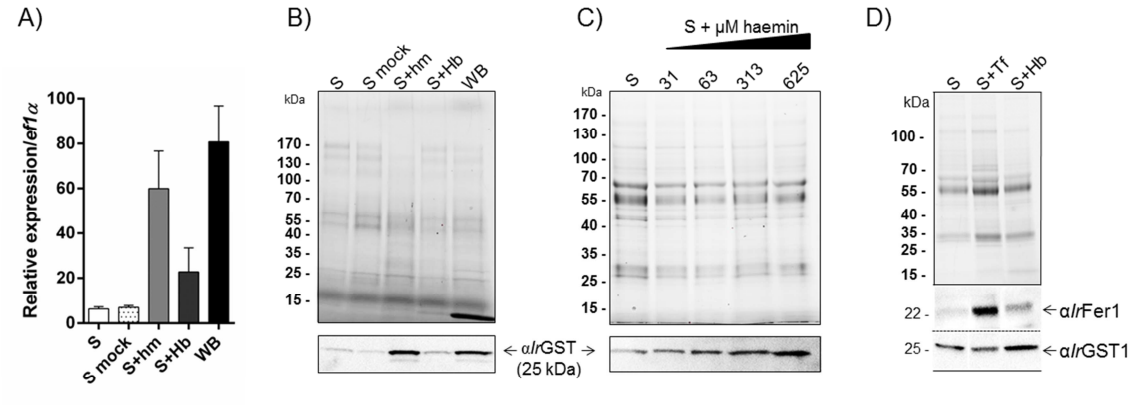

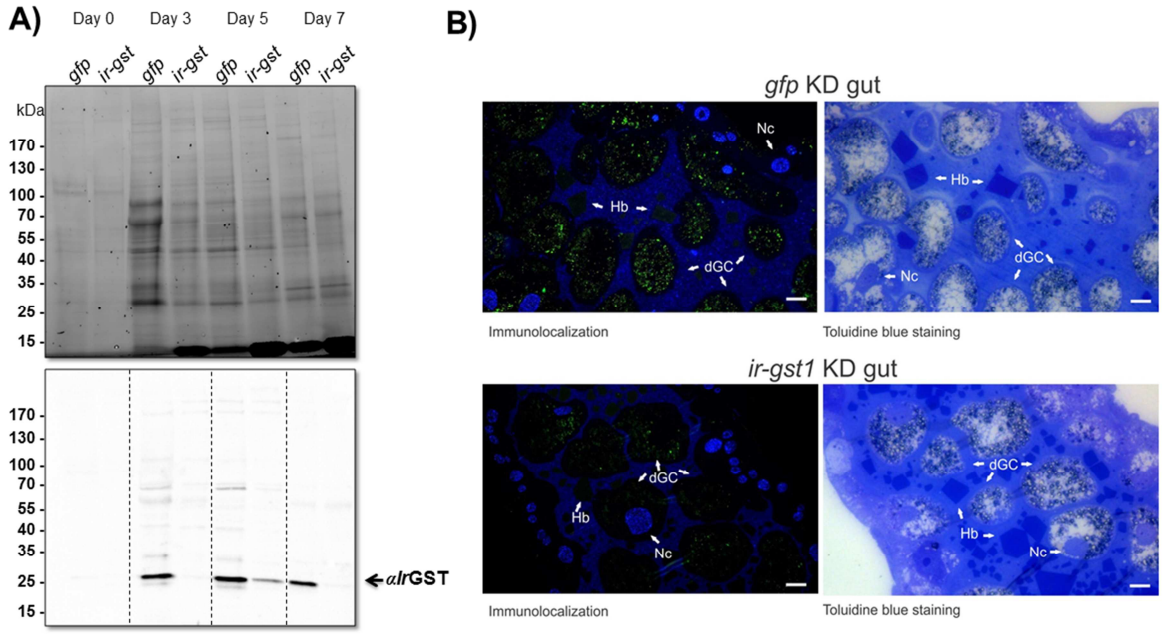
A)
Day 0
Day 3
Day 5
Day 7
gfp
ir-gst
kDa
170
130
100
70
55
40
35
25
15
αIrGST
B)
gfp KD gut
Nc
Hb
dGC
Immunolocalization
Toluidine blue staining
ir-gst1 KD gut

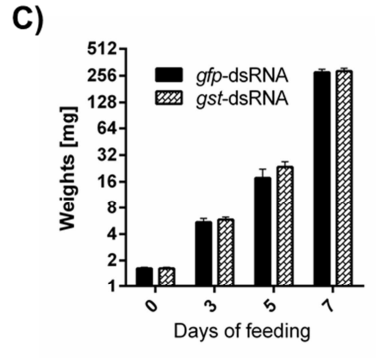
C)
512
256
128
64
32
16
8
4
2
1
Weights [mg]
gfp-dsRNA
gst-dsRNA
0
3
5
7
Days of feeding

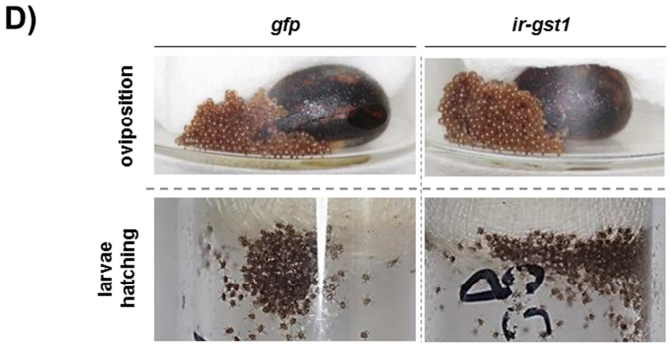
D)
gfp
ir-gst1
oviposition
larvae hatching

A)

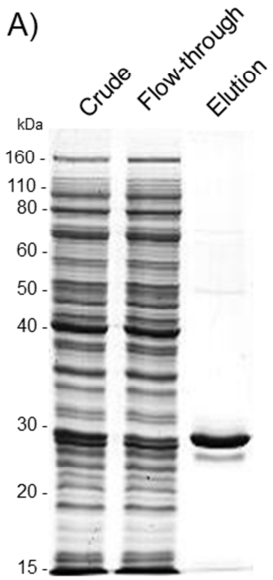

B)

Specific activities with selected substrates (nmol substrate / min / mg protein)

	I. ricinus	*F. hepatica*
CDNB	1820 ± 77	2451 ± 115
T2N	0	150 ± 8
C-HPx	1567 ± 35	915 ± 95

C)

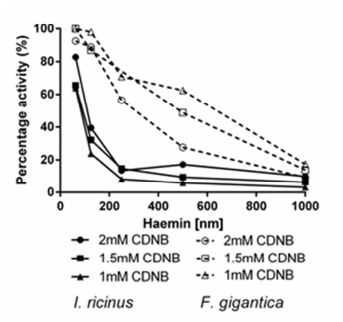

D)

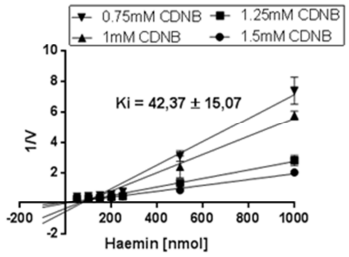

E)

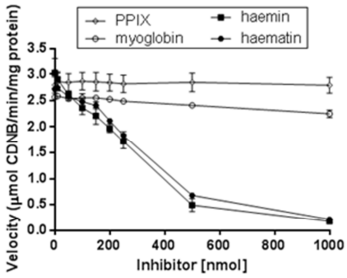

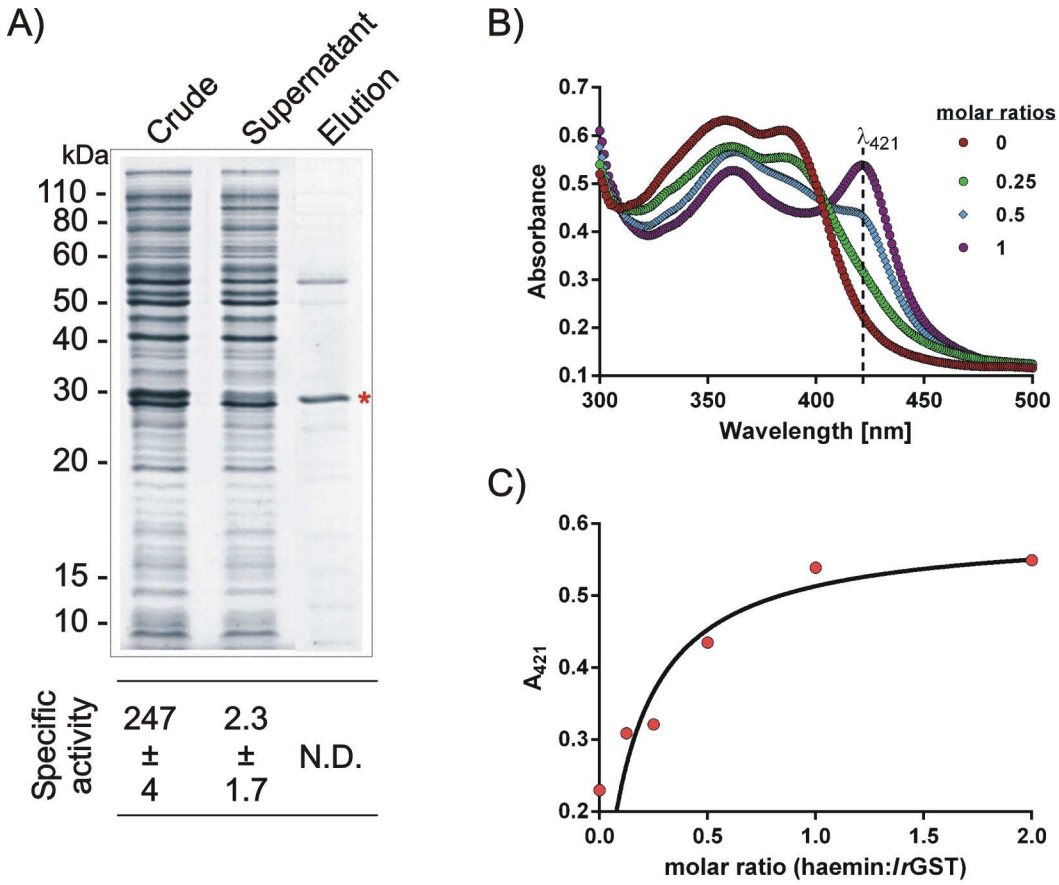

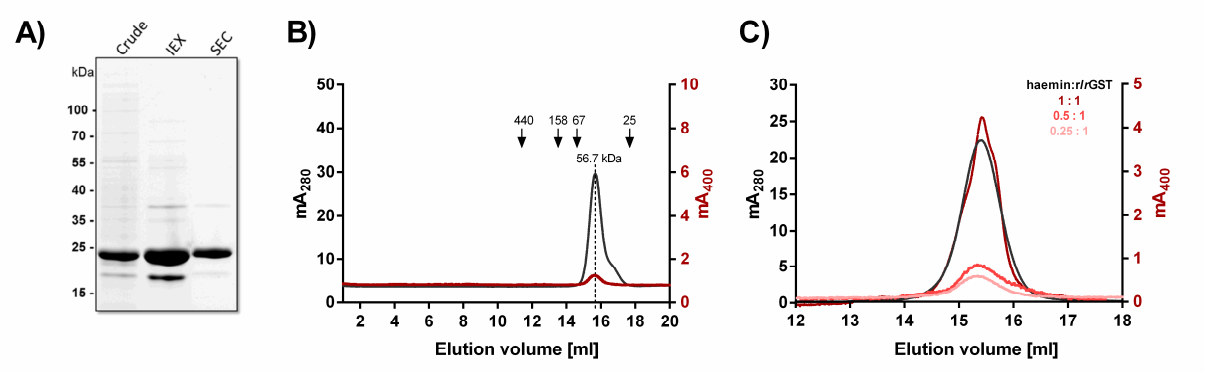

Highlights

- Haem-inducible *Ir*GST1 from *Ixodes ricinus* is the first functionally characterised tick GST of delta-/epsilon-class
- *Ir*GST1 and its orthologues from other ticks form a phylogenetically distinct clade of GSTs that secondarily acquired haem-binding properties
- *ir-gst1* tick gut expression is induced by host haem, but not by host iron
- *Ir*GST1binds haemin *in vitro* and is presumably an endogenous intracellular scavenger of excessive haem